Article

pubs.acs.org/Biomac

Glycine-Terminated Dendritic Amphiphiles for Nonviral Gene Delivery

Shashwat Malhotra,[†] Hannah Bauer,[‡] Ariane Tschiche,[†] Anna Maria Staedtler,[†] Andreas Mohr,[†] Marcelo Calderón,[†] Virinder S. Parmar,[§] Lena Hoeke,[‡] Soroush Sharbati,[‡] Ralf Einspanier,*[,‡] and Rainer Haag*[,†]

[†]Institut für Chemie und Biochemie, Freie Universität Berlin, Takustrasse 3, Berlin 14195, Germany

[‡]Institute of Veterinary Biochemistry, Freie Universität Berlin, Oertzenweg 19b, Berlin 14163, Germany

[§]Bioorganic Laboratory, Department of Chemistry, University of Delhi, Delhi 110 007, India

Supporting Information

ABSTRACT: Development of nonviral vectors for the successful application of gene therapy through siRNA/DNA transfection of cells is still a great challenge in current research.[1,2] In the present study, we have developed multivalent polyglycerol dendron based amphiphiles with well-defined molecular structures that express controlled glycine arrays on their surfaces. The structure−activity relationships with respect to the siRNA complexation, toxicity, and transfection profiles were studied with synthesized amphiphilic polycations. Our findings revealed that a second-generation amphiphilic dendrimer (G2-octaamine, **4**) that has eight amine groups on its surface and a hydrophobic C-18 alkyl chain at the core of the dendron, acts as an efficient vector to deliver siRNA and achieve potent gene silencing by investigating the knockdown of luciferase and GAPDH gene activity in HeLa cells. Interestingly, the amphiphilic vector is nontoxic even at higher ratio of N/P 100. To the best of our knowledge this is the first example of successful in vitro siRNA transfection using dendritic amphiphiles. We believe that this supramolecular complex may serve as a new promising alternative for nonviral siRNA delivery systems and will be investigated for in vivo siRNA delivery in the future.

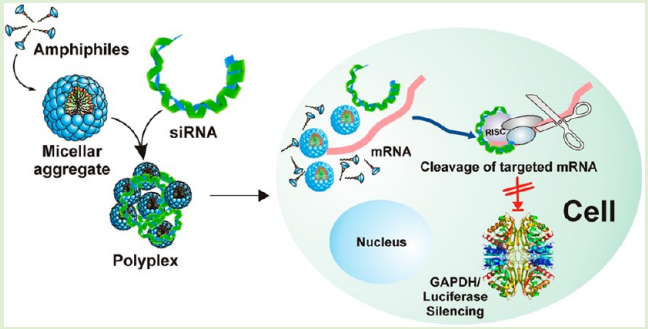

INTRODUCTION

Gene therapy has gained significant attention over the past two decades as a potential method for treating chronic diseases and genetic disorders as well as an alternative method to traditional chemotherapy for cancer treatment.[1−3] A considerable amount of research effort is currently being focused on designing effective gene vectors that can condense and protect oligonucleotides for gene transfection, whereby free oligonucleotides and DNA are rapidly degraded by serum nucleases in the blood when injected intravenously and therefore cannot easily pass through the negatively charged cell surface barrier.[4] Earlier research concentrated on using viral gene vectors, including both retro- and adenoviruses, as these vectors have exhibited high gene transfection efficiency by delivering both DNA and RNA to numerous cell lines.[5] Elementary problems including toxicity, inflammatory, immunogenic, and mutagenic effects, however, make them a safety risk and underline the urgent need for nonviral alternatives.[6]

Nonviral gene delivery vector systems, including cationic lipids,[7] polymers,[8] dendrimers,[9] and peptides,[10] are frequently regarded as a potentially safer alternative to viral gene delivery. However, unlike viral analogues that have developed means to overcome cellular barriers and immune defense mechanisms, nonviral gene carriers often exhibit significantly reduced transfection efficiencies as they are stalled by numerous extra- and intracellular obstacles. However, biocompatibility, ease, and potential for large-scale production make these compounds increasingly attractive for gene therapy.[11] As a result, a significant amount of research in the past decade has been focused on designing cationic compounds that can form complexes with DNA and overcome in vitro and in vivo barriers for gene delivery. Among them, dendrons have been of particular interest as a result of their ability to deliver genetic material into the cells.[12] Because of the multivalency effect, dendrons can have multiple densely packed surface groups that offer multiple simultaneous interactions that lead to enhanced binding.[13,14] Ever since the ground-breaking work from the groups of Tomalia and Szoka using poly(amidoamine) spherical dendrimers, a wide range of different dendritic architectures have been explored for their gene delivery potential.[15,16] In most cases, large polycationic dendrimers based on polyamines such as dendritic poly-L-lysine and

Received: June 12, 2012
Revised: July 30, 2012
Published: August 10, 2012

polyglycerol amines have been employed.[17−26] Such systems can be considered to belong to the cationic polymer class of gene delivery vehicle. Although such systems can perform highly effective gene delivery, they also exhibit challenging toxicity profiles and can cause problems as a result of their persistence inside the cells after gene delivery has taken place.[27,28] A different approach has therefore been to use dendron based architectures in which a hydrophobic group at the focal point (amphiphiles) encourages self-assembly of the dendrons into a larger aggregate, "pseudodendrimer". Such systems, as reported by different research groups, are not only capable of condensing the genetic materials but also for delivering and silencing the cells.[29−33] Based on their amphiphilic nature, such dendrons are considered to belong to the cationic lipid class for gene delivery vehicle.[34,35] In contrast to most phospholipid based vesicles, these dendritic glycerol amphiphiles form defined and shape persistant micelles.[36]

Our interest is in optimizing siRNA binding and delivery into cells by developing low-molecular-weight oligoglycerol based amphiphiles with low cellular toxicity. We therefore decided to develop multivalent amphiphiles with well-defined molecular structures that express controlled multivalent glycine arrays on their surfaces. These amino acids are naturally occurring building blocks and can be used as biodegradable amine-functionalities. Our endeavor was to control the loading of amine content on the surface of the dendritic head-groups of the synthesized amphiphiles using chemo-enzymatic and classical chemical synthetic routes. Such systems enable an understanding of structure−activity relationships with respect to the siRNA complexation, toxicity, and transfection profiles often associated with amine bearing polycations. Here, we present a second-generation amphiphilic dendrimer (G2-octaamine, **4**) with eight amine groups on its surface and a C-18 hydrophobic alkyl chain at the core that acts as an efficient vector to deliver siRNA and achieve potent gene silencing by investigating the knockdown of a luciferase gene in stably transfected HeLa cells as well as knockdown of the intrinsic expression of GAPDH in HeLa cells. To the best of our knowledge, this is the first example of successful in vitro siRNA transfection using dendritic amphiphiles. It may represent a promising nonviral carrier system for siRNA delivery with a clear in vivo application potential.

EXPERIMENTAL SECTION

Materials. Air and moisture sensitive reactions were carried out in flame-dried glass ware under argon atmosphere. Anhydrous solvents were either commercially purchased from Acros Organics™ in septum-sealed bottles or chemically dried using a MBRAUN SPS 800 solvent purification system. Shell acetal-protected PG dendrons [G1.0]−OH (**5**) and [G2.0]−OH (**10**) were provided by our group. Mono-*Boc*-protected glycine was supplied by the Acros Organics. All other chemicals were of reagent grade quality and used without further purification from the suppliers Acros Organics, Fluka, Sigma-Aldrich, Roth, Invitrogen, and Merck.

Measurements. *Chromatography and Spectroscopy.* Thin layer chromatography (TLC) analysis was carried out on silica coated aluminum plates from Merck either using silica gel 60, F_{254}, or silica gel 60 RP-18 F_{254}s when performing reversed phase (RP) analysis. Preparative column chromatography was conducted on silica gel 60 (0.040−0.063 mm, 230−400 mesh ASTM). Detection was accomplished by UV irradiation (254 nm; 366 nm) and different staining solutions such as potassium permanganate, cerium molybdate, ninhydrin, bromocresol green, and Dragendorff reagent.

NMR spectra were recorded on a Bruker ECX 400 (^{1}H: 400 MHz, ^{13}C: 100.5 MHz), a Jeol Eclipse (^{1}H: 500 MHz, ^{13}C: 125.8 MHz), or on a Bruker Biospin (^{1}H: 700 MHz, ^{13}C: 176.1 MHz) spectrometer at 25 °C and calibrated against residual solvent peaks as internal standard. All ^{13}C NMR spectra were recorded with ^{1}H broadband decoupling. Chemical shifts δ are given in ppm according to calibration to the corresponding solvents $CDCl_3$ (^{1}H: 7.26 ppm, ^{13}C: 77.00 ppm) and CD_3OD (^{1}H: 3.31 ppm, ^{13}C: 49.05 ppm). Electrospray-ionization time-of-flight mass spectrometry (ESI-TOF-MS) experiments were carried out on an Agilent 6210 ESI-TOF, Agilent Technologies.

Critical Micelle Concentration (CMC). Fluorescence emission spectra were taken with a Jasco FP-6500 spectrofluorimeter equipped with a thermostatted cell holder, a DC-powered 150 W xenon lamp, a Hamamatsu R928 photomultiplier, and a variable slit system. Both excitation and emission slits were set at 5 nm. In the present study, diphenyl-1,3,5-hexatriene (DPH) was used as a hydrophobic probe to determine the critical micelle concentrations (CMCs) of the amphiphiles in buffered aqueous solution (HEPES saline buffer, 9.4 mM NaCl, pH 7.2). Fluorescence of DPH was recorded from 360 to 600 nm after excitation at 345 nm. In order to determine the CMCs, the fluorescence intensity of the most intensive peak at 430 nm was plotted against the amphiphile concentration. Independent linear regressions were performed on the data points above and below the putative CMC.[37−40] The CMCs were derived from the points of intersection of the independent linear regressions.

Prior to measurements, DPH stock solution of 0.5 μM (in HEPES saline buffer, 9.4 mM NaCl, pH 7.2) was freshly prepared by dissolving the probe in THF or acetonitrile. Increasing concentrations of amphiphiles were then added to DPH (0.5 μM) from a stock solution and fluorescence emission spectra were measured at different amphiphile concentrations. To ensure proper mixing and dissolution of the compounds all samples were stirred thoroughly by using a laboratory vortex shaker. The samples were then incubated for at least 12 h at room temperature. All measurements were carried out at 22 ± 2 °C and taken in triplicate and averaged. Data analysis was performed using SigmaPlot 8.0 software.

Dynamic Light Scattering (DLS) and Zeta Potential. DLS and zeta potential measurements were conducted at 25 °C using a Zetasizer Nano ZS analyzer with integrated 4 mW He−Ne laser, λ = 633 nm (Malvern Instruments Ltd., U.K.). The amphiphiles were measured in HEPES saline buffer (2 mM, EDTA 10 μM, NaCl 9.4 mM) at a pH of 7.2. Lipopolyplex solutions were obtained as follows: first a 200 μM DNA (21-mer oligonucleotides) solution was freshly prepared in the relevant buffer solution. With respect to a certain N/P ration, the appropriate amount of amphiphile was added. Here, it should be noted that the final concentrations of the respective amphiphiles were above each CMC. After mixing and incubation for 30 min, the sample solutions were directly measured. All measurements were carried out using folded capillary cells (DTS 1060) in three replicate measurements.

Ethidium Bromide Assay. The experimental protocol for the ethidium bromide (EthBr) displacement assay was based on a previously reported study.[41] Fluorescence spectroscopy measurements were performed with a JASCO FP-6500 spectrofluorometer. Excitation of the sample was done with 546 nm excitation light, and emission was measured from 560 to 700 nm. We studied the DNA-binding properties at low salt concentration in HEPES saline buffer (pH 7.2, 2 mM HEPES, 9.4 mM NaCl). A total of 0.1242 mg of EthBr was dissolved in 50 mL of buffer to provide 1.26 μM concentration. In order to prepare 100 mL of a 5 μM solution of DNA (21-mer oligonucleotides), 0.0762 mg of each strand of DNA was measured in an accurate scale. For preparation of double helix, incubation was done by keeping strands at 90 °C for 1 min and then 2 h at 37 °C. DNA was provided from Operon Biotechnologies GmbH. Mother solutions (1000 μM based on nitrogen content) for each tested amphiphile were prepared in buffer solution. Solutions containing DNA and EthBr in buffer were first incubated at room temperature for 5 min to ensure interaction. The fluorescence of the DNA solution with EthBr was set at 100%. Consequently, an appropriate quantity of the corresponding amphiphile was added in order to reach the desired N/P ratio followed

by further incubation for 5 min, after each addition. Here, it should be noted that the final concentrations of the respective amphiphiles were above each CMC. Control experiments were also conducted by measuring solutions which only contained EthBr and the amphiphiles. Results were normalized against the set 100% value and expressed as a percentaged reduction of the relative fluorescence intensity.

Agarose Gel Electrophoresis. One day prior to electrophoresis the glycine amphiphiles were dissolved in ddH_2O. Complexes of glycine amphiphiles and fluorescently labeled siRNA (FAM-siRNA, GUCAACGGAUUUGGUCGUA, Eurogentec) were created by incubation for 30 min at room temperature. They were loaded on 4% high-resolution agarose gels (MetaPhor Agarose, Lonza) and subjected to electrophoresis at 70 V. Polymer-FAM-siRNA-complexes were visualized after excitation at 495 nm and acquiring the emitted fluorescence signal at 520 nm using the Fusion SL imager (Vilber Lourmat).

Cell Culture and Treatment. Two human cell lines HeLa (ATCC No. CCL-2) and HeLa-Luc (provided by Biontex Laboratories GmbH, constitutively expressing the firefly luciferase) were cultured at 37 °C and 5% CO_2 either in RPMI 1640 or DMEM (Biochrom AG) with 1.5 g/L $NaHCO_3$ both supplemented with 10% fetal bovine serum. Cells were grown in 96-well plates (6×10^4 cells per well) for 24 h and transfected using the glycine amphiphiles and Lipofectamine 2000 transfection reagent (Invitrogen) as control. One day before transfection the glycine amphiphiles were dissolved in ddH_2O. Depending on the following experiments different double-stranded siRNA molecules were used.

Intracellular Uptake. For the determination of transfection efficiency of each glycine amphiphile the intracellular siRNA-uptake was measured using fluorescently labeled nonsense siRNA (Cy3 dye-Labeled Pre-miR Negative Control #1 - Life Technologies). 48 h after transfection, efficiency of delivery was analyzed by fluorescence microscopy.

Cell Viability Assays. Cytotoxicity and cell viability were measured using a colorimetric WST-1 assay (Roche) and the xCELLigence system (Roche) to monitor cell index profiles and determining cell counts, proliferation and cytotoxicity. Both assays were performed in 96-well plates (6×10^4 cells per well). Each plate contained blanks, controls (negative and positive), and substance dilution series with four replicates. Nontargeting siRNA (ON-TARGETplus nontargeting pool, D-001810-10, Thermo Fisher Scientific) transfection was accomplished and WST-1 assay was performed according to the manufacturer's instructions.

RNA Interference and Transient Transfections. siRNAs targeting GAPDH (ON-TARGETplus GAPD Control siRNA, D-001830-01, Thermo Fisher Scientific) or Luciferase (CUUACGCUGAGUACUUCGA, Eurofins MWG Operon) and nontargeting siRNA (Thermo Fisher Scientific) as a control were used for performing the transient transfections. As positive control for transfection, the reagent Lipofectamine 2000 was used following the manufacturer's protocol. siRNA-transfection-reagent-complexes were prepared by incubating 5 pmol siRNA with various amounts of aqueous glycine amphiphiles depending on N/P ratios in OptiMEM (Gibco) for 30 min. Thereafter, the siRNA-transfection-reagent-complexes were added to the cells. Both were incubated for at least 48 h at 37 °C and 5% CO_2. Samples were taken after transfection for RNA extraction or luciferase assays.

RNA isolation was performed with the NucleoSpin RNA XS Kit (Macherey-Nagel). Determination of RNA quality and RT-qPCR assays were performed as described previously[42] and the normalization of the gene of interest (GAPDH; Gene ID: 2597; forward: 5′-CCATCTTCCAGGAGCGAGAT-3′; reverse: 5′-CTAAGCAGTTGGTGGTGCAG-3′) was performed using geNorm.[43] In this study B2M (Gene ID: 567; forward: 5′-TGCTGTCTCCATGTTTGATGTATCT-3′; reverse: 5′-TCTCTGCTCCCCACCTCTAAGT-3′), SDHA (Gene ID: 6389; forward: 5′-TGGGAACAAGAGGGCATCTG-3′; reverse: 5′-CCACCACTGCATCAAATTCATG-3′), and ACTB (Gene ID: 60; forward: 5′-GGACTTCGAGCAAGAGATGG′3; reverse: 5′-AGCACTGTG TTGGCGTACAG-3′) were used as housekeeping genes.

For normalization of luciferase assays, cells were treated with Calcein AM (Sigma Aldrich) to quantify the amount of viable cells. After uptake of Calcein AM by living cells and acetoxymethyl ester hydrolysis by cellular esterases, fluorescence is detected only in viable cells, which enables the estimation of cell viability in a population. For this purpose, the cell culture medium was removed and cells were washed with PBS (PAA) and incubated with fresh medium containing 4 mM Calcein AM for 30 min at 37 °C and 5% CO_2. After removal of medium 100 μL PBS per well were added and fluorescence was measured by excitation at 485 nm and acquiring the emission at 520 nm using the FLUOStar OPTIMA (BMG Labtech). An additional washing step with PBS was done and 20 μL of lysis-juice (PJK GmbH) per well was added. Measuring of luciferase activity was performed according to the manufacturer's manual.

In Vivo Toxicity. Three BALB/c mice per group were treated intravenously (i.v.) with 8, 20, and 40 mg/kg G2-octaamine (**4**) complexed with nontargeting siRNA (ON-TARGETplus Nontargeting siRNA #1, Dharmacon) at N/P ratios of 50, 70, and 100, respectively. HiPure water was administered i.v. as control. Retrobulbar blood was taken 1 h after administration. Cytokine levels in the blood were evaluated using the Meso Scale Discovery Multi-Spot Assay System, Mouse ProInflammatory 7-Plex Assay Ultra-Sensitive Kit.

Synthesis of Compounds 5−8. The synthesis of compounds **5**, **6**, **7**, and **8** were performed according to our previous report.[44]

General Procedure for the Esterification of Compounds 8 and 13. *N*-boc glycine (2.66 mmol), 4-(dimethylamino)pyridine (20.0 mg), and the relavent compounds **8** (0.332 mmol) and **13** (0.166 mmol) were dissolved in 15 mL of DMF and cooled to 0 °C under ice bath. l-Ethyl-3-[3-(dimethylamino) propyl]carbodiimide hydrochloride (EDCI, 2.66 mmol) along with a few drops of triethyl amine were added and the reaction mixture was stirred first at 0 °C for 2 h and then at room temperature, overnight. The solution was concentrated to dryness in vacuum, and the residue was taken up in chloroform (25 mL) and water (5 mL). The organic layer was separated, washed with saturated sodium bicarbonate (2 × 15 mL) and water (2 × 15 mL), and dried over $MgSO_4$. The solvent was removed in vacuum, and the products **9** and **14** were purified by column chromatography (chloroform/methanol, 95:5) as viscous oils.

Compound 9. Obtained as light yellow viscous oil (318 mg, 78% yield). ^{1}H NMR (400 MHz, methanol-d_4) δ 0.83−0.88 (3H, t, J = 8.0 Hz, $-CH_3$), 1.24 (30H, s, methylene protons), 1.40 (36H, s, $-C(CH_3)_3$), 1.51−1.59 (2H, m, $-O-CH_2CH_2$-), 3.24−3.28 (2H, m), 3.45−3.50 (2H, m, PG dendron), 3.56−3.63 (3H, m, PG dendron), 3.73 (8H, s, $-CO-CH_2$-NHBoc), 3.86−3.93 (4H, m, PG dendron), 4.12−4.25 (4H, m, PG dendron), 4.54 (2H, s), 5.14−5.18 (2H, m, PG dendron), 7.97−8.00 (1H, m, Triazole-H); ^{13}C NMR (100.5 MHz, methanol-d_4) δ 15.61, 24.87, 26.39, 28.36, 29.90, 31.61, 31.78, 31.92, 34.20, 44.07, 44.19, 50.97, 63.20, 65.01, 65.77, 71.45, 72.20, 72.95, 73.17, 81.72, 126.26, 146.90, 159.46, 172.59, 172.85. HRMS: m/z Calcd for $C_{58}H_{103}N_7O_{19}Na$: 1224.7223 $[M+Na]^+$. Found: 1224.7373. (For ^{1}H and ^{13}C NMR spectra, see the Supporting Information.)

General Procedure for the Boc-Deprotection of Compounds 9, 14, and 15. Compounds **9**, **14**, and **15** (100 mg) were treated overnight with a mixture of trifluoroacetic acid/dichloromethane (1:3). The reaction mixture was evaporated under reduced pressure to afford the tetra, octa, and diamino compounds **3**, **4**, and **16**, respectively, as viscous oils.

Compound 3. Obtained as colorless viscous oil (104 mg, quant. yield). ^{1}H NMR (400 MHz, methanol-d_4) δ 0.87 (3H, t, J = 6.9 Hz), 1.26 (30H, s, methylene protons), 1.56−1.62 (2H, m, $-O-CH_2CH_2$-), 3.52 (2H, t, J = 6.7 Hz), 3.58−3.65 (2H, m, PG dendron), 3.67−3.76 (2H, m, PG dendron), 3.85 (8H, s, $-CO-CH_2$-NHBoc), 3.87−4.01 (5H, m, PG dendron), 4.23−4.27 (2H, m, PG dendron), 4.39−4.41 (2H, m, PG dendron), 4.57 (2H,s), 5.23−5.31 (2H, m, PG dendron), 7.95 (1H, s, Triazole-H); ^{13}C NMR (100.5 MHz, methanol-d_4) δ 13.12, 22.40, 25.86, 26.40, 29.14, 29.29, 29.46, 30.37, 31.74, 35.69, 39.59, 39.71, 63.22, 63.46, 68.52, 69.85, 70.68, 71.84, 113.28 (TFA), 116.21 (TFA), 123.73, 144.72, 160.24, 160.61, 166.88, 167.08. HRMS: m/z Calcd for $C_{38}H_{72}N_7O_{11}$: 802.5284 $[M+H]^+$. Found:

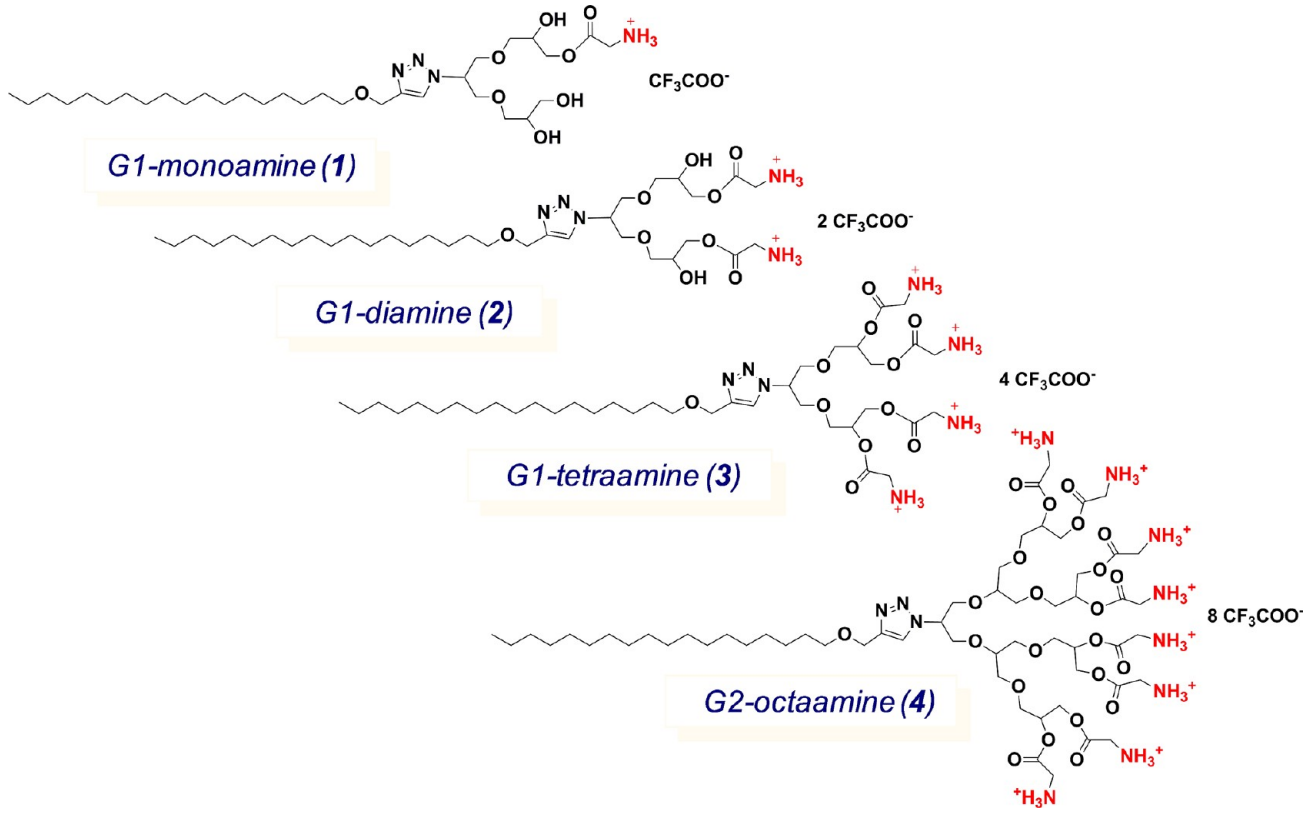

Figure 1. Structures of the PG-amphiphiles investigated in this paper.

802.5295. (For ^{1}H and ^{13}C NMR spectra, see the Supporting Information.)

Procedure for the Synthesis of Compounds 10 and 11. The synthesis of compounds **10** and **11** were performed according to our previous report.[45]

Compound ***12***. Compound **11** (1.00 g, 1.38 mmol, 1 equiv), 1-prop-2-ynyloxy-octadecane (0.47 g, 1.52 mmol, 1.1 equiv), DIPEA (0.14 mL, 0.83 mmol, 0.6 equiv), and bromotris (triphenylphosphine)-copper(I) (0.26 g, 0.28 mmol, 0.2 equiv) were dissolved in dry THF and the reaction mixture was left for stirring at 40 °C for 16 h. Since TLC analysis did not indicate full consumption of the starting material (generally at any point of time), the reaction mixture was treated with saturated EDTA solution. Before doing so, the solvent was evaporated and the residue dissolved in DCM. After aqueous workup the solvent was removed under reduced pressure. The resulting residue was then subjected to the same reaction conditions as initially employed including also the same amounts of reactants referred to DIPEA, Cu catalyst and THF. After completion of reaction, the mixture was evaporated and again extracted with saturated EDTA solution in the same manner as above-mentioned in order to remove any traces of copper ions. The resulting crude product was purified by column chromatography ($CHCl_3$/MeOH, 99:1) yielding compound **12** as yellowish viscous oil (0.91 g, 64%).

^{1}H NMR (700 MHz, $CDCl_3$): δ 0.87 (t, J = 7.1 Hz, 3 H, alkyl CH_3), 1.24 (br s, 30 H, methylene CH_2), 1.34 (br s, 12 H, acetal CH_3), 1.39 (br s, 12 H, acetal CH_3), 1.58 (m$_c$, 2 H, CH_2-CH_2−O), 3.65−3.38 (m, 20 H, PG dendron), 3.68 (m$_c$, 4 H, PG dendron), 3.88 (m$_c$, 2 H, CH_2−CH_2-O), 4.02 (m$_c$, 6 H, PG dendron), 4.24−4.16 (m, 4 H, PG dendron), 4.59 (s, 2 H, O−CH_2-trz), 4.85 (m$_c$, 1 H, PG dendron), 7.73 (m$_c$, 1 H, trz); ^{13}C NMR (176 MHz, $CDCl_3$): δ 14.2, 22.8, 25.5, 26.3, 26.9, 29.5, 29.7, 29.8, 32.1, 61.0, 64.5, 66.8, 66.9, 69.5, 70.4, 71.1, 71.3, 71.4, 71.6, 71.7, 71.8, 72.7, 74.8, 74.9, 78.6, 78.9, 109.5, 122.9, 145.1. HRMS: m/z Calcd for $C_{54}H_{99}N_3O_{15}Na$: 1052.6974 $[M+Na]^+$. Found: 1052.7005.

Compound ***13***. Acidic ion-exchange resin Dowex (200 mg) and a few drops of water were added to a solution of compound **12** (400 mg, 0.388 mmol) in methanol (5 mL) and stirred overnight at refluxing temperature. After TLC analysis, dowex was filtered off and the solvent was evaporated in vacuum. After column chromatography of the obtained residue, pure product was obtained as a white sticky solid (280 mg, 83%).

^{1}H NMR (700 MHz, CD_3OD): δ 0.97 (t, J = 7.1 Hz, 3 H, CH_3), 1.35 (br s, 30 H, methylene CH_2), 1.66 (quint, J = 7.8 Hz, 2 H, CH_2-CH_2−O), 3.65−3.46 (m, 24 H, PG dendron), 3.68 (m$_c$, 2 H, CH_2−CH_2-O), 3.84−3.73 (m, 5 H, PG dendron), 4.22−3.97 (m, 5 H, PG dendron), 4.65 (s, 2 H, O−CH_2-trz), 5.04 (m$_c$, 1 H, PG dendron), 8.18 (m$_c$, 1 H, trz); ^{13}C NMR (176 MHz, CD_3OD): δ 14.4, 23.7, 27.2, 30.5, 30.6, 30.7, 30.8, 33.1, 62.8, 64.4, 79.7, 64.5, 64.7, 70.4, 70.5, 71.4, 71.8, 72.1, 72.2, 72.4, 72.5, 72.8, 72.9, 74.0, 80.0, 125.3, 145.7. HRMS: m/z Calcd for $C_{42}H_{83}N_3O_{15}Na$: 892.5722 $[M+Na]^+$. Found: 892.5742.

Compound ***14***. Obtained as colorless viscous oil (246 mg, 70% yield). ^{1}H NMR (400 MHz, $CDCl_3$) δ 0.82−0.91 (3H, m, −CH_3), 1.24 (30H, s, methylene protons), 1.43 (72H, s, −$C(CH_3)_3$), 1.54−1.62 (2H, m, −O−CH_2CH_2-), 3.38−3.67 (19H, m, PG dendron and −O-CH_2CH_2−), 3.87 (16H, s, −CO−CH_2-NHBoc), 3.96−4.01 (2H, m, PG dendron), 4.17−4.39 (8H, m, PG dendron), 4.47 (4H, m, PG dendron), 4.59−4.61 (2H, m), 5.20−5.28 (4H, m, PG dendron), 7.74 − 7.79 (1H, m, Triazole-H); ^{13}C NMR (100.5 MHz, $CDCl_3$) δ 14.01, 22.60, 26.07, 27.80, 28.29, 29.27, 29.62, 31.85, 42.30, 63.07, 63.86, 68.34, 69.37, 70.83, 71.19, 78.51, 79.87, 84.63, 122.63, 144.76, 155.95, 169.94, 170.21. HRMS: m/z Calcd for $C_{98}H_{171}N_{11}NaO_{39}$: 2150.1667 $[M+Na]^+$. Found: 2150.1705. (For ^{1}H and ^{13}C NMR spectra, see the Supporting Information.)

Compound ***4***. Obtained as colorless viscous oil (105 mg, quant. yield). ^{1}H NMR (500 MHz, $CDCl_3$) δ 0.85−0.92 (3H, m, −CH_3), 1.28 (30H, s, methylene protons), 1.56−1.64 (2H, m, −O−CH_2CH_2-), 3.42−3.76 (22H, m, PG dendron and −O-CH_2CH_2−), 3.81−3.84 (1H, m, PG dendron), 3.89 and 3.91 (16H, 2s, −CO−CH_2-NHBoc), 3.99−4.10 (2H, m, PG dendron), 4.30−4.42 (4H, m, PG dendron), 4.47−4.56 (4H, m, PG dendron), 4.55−4.61 (2H, m), 5.24−5.37 (4H, m, PG dendron), 8.04 (1H, s, Triazole-H); ^{13}C NMR (176 MHz, MeOD) δ 12.77, 22.47, 25.10, 25.87, 26.41, 29.02, 29.30, 31.64, 39.53,

dx.doi.org/10.1021/bm300892v | *Biomacromolecules* 2012, 13, 3087−3098

Scheme 1. Synthesis of G1-Tetraamine (3)

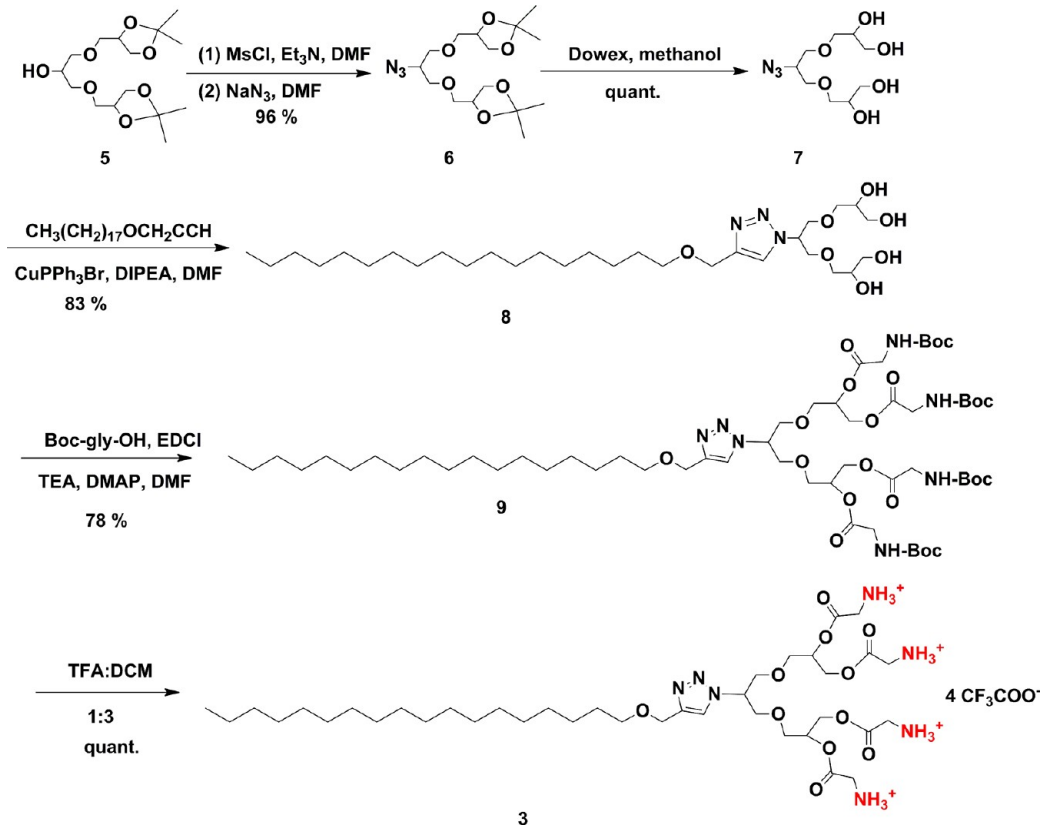

Scheme 2. Synthesis of G2-Octaamine (4)

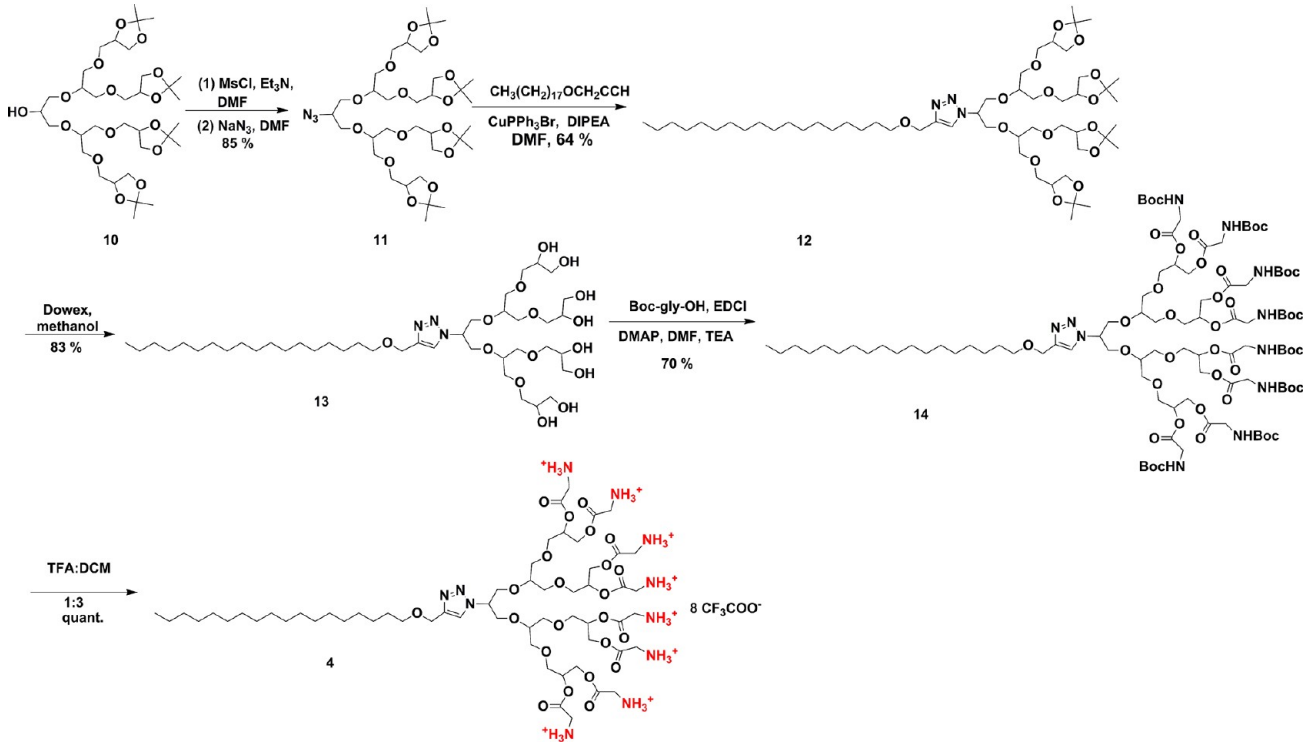

63.09, 63.60, 67.57, 68.63, 70.72, 72.00, 78.55, 115.52 (TFA), 117.17 (TFA), 124.74, 144.38, 160.89, 167.01. HRMS: *m/z* Calcd for $C_{58}H_{107}N_{11}NaO_{23}$: 1348.7439 $[M+Na]^+$. Found: 1348.7443. (For ^1H and ^{13}C NMR spectra, see the Supporting Information.)

Compound 15. Compound **15** was synthesized according to our previously reported procedure.[44]

Compound 16. Obtained as light yellow viscous oil (102 mg, quant. yield). ^1H NMR (500 MHz, MeOD) δ 3.53–3.60 (6H, m), 3.67–3.77 (4H, m), 3.87 (4H, s), 3.99–4.01 (1H, m), 4.24–4.28 (2H, m), 4.34

dx.doi.org/10.1021/bm300892v | *Biomacromolecules* 2012, 13, 3087–3098

(2H, dd, J = 11.3, 3.9 Hz); ^{13}C NMR (126 MHz, MeOD) δ 39.73, 60.17, 60.69, 66.91, 67.87, 70.79, 71.86, 114.78 (TFA), 117.08 (TFA), 159.85 (TFA), 167.14. HRMS: m/z Calcd for $C_{13}H_{26}N_5O_8$: 380.1770 $[M+H]^+$. Found: 380.1777.

RESULTS AND DISCUSSION

Synthesis. In order to correlate the number of amine functionalities on the surface of the PG dendron based amphiphiles with respect to siRNA complexation, delivery, toxicity, and transfection, we decorated the surface of bifunctional dendrons with different degrees of glycine loadings in the shell and a C-18 hydrophobic alkyl chain at the focal point. Thus, by controlling the number of amine functionalization on the surface of PG-amphiphiles of generation 1 and 2, viz. G1-monoamine (**1**), G1-diamine (**2**), G1-tetraamine (**3**), and G2-octaamine (**4**) were synthesized (Figure 1). The aminated compounds **1**−**4** were synthesized using facile chemoenzymatic and classical organic synthesis. G1-monoamine (**1**) and G1-diamine (**2**) were synthesized according to our previously reported procedure.[44]

For the synthesis of G1-tetraamine (**3**), we had first prepared the deprotected amphiphile **8** according to our previous report.[44] Starting from [G1.0]−OH (**5**), the free secondary hydroxyl group of [G1.0]−OH (**5**) was converted to the corresponding mesylate and without further purification treated with sodium azide to give [G1.0]−N3 (**6**) in 96% yield over two steps (Scheme 1). The acetal protecting groups of compound **6** were removed in 90% yield by refluxing with an acidic ion-exchange resin in methanol to obtain compound **7**. We then performed the click reaction on compound **7** with octadecyl-propargylether using copper triphenylphosphine bromide, diisopropylethylamine and *N*,*N*-dimethylformamide as a solvent at 50 °C for 24 h to afford G1 click amphiphile **8** in 83% yield. The hydroxyl groups of G1 click amphiphile **8** were then decorated via esterification, using *N*-Boc-glycine as the acylating agent in the presence of condensation reagent EDCI and DMAP as a base at room temperature in DMF solvent to furnish tetra boc-protected compound **9** in 78% isolated yield (Scheme 1). Tetra boc-protected compound **9** was then treated overnight with a mixture of trifluoroacetic acid/dichloromethane (1:3) to afford G1-tetraamine (**3**), in quantitative yield as trifluoroacetate salt (Scheme 1).

Regarding the synthesis of G2-octaamine (**4**) (Scheme 2), we had first prepared the compound [G2.0]−OH (**10**) according to our previous report.[45] As described above, the free secondary hydroxyl group of [G2.0]−OH (**10**) was also converted to the corresponding mesylate and without further purification treated with sodium azide to give [G2.0]−N3 (**11**) in 85% yield over two steps. We then carried out the click reaction on compound **11** with octadecyl-propargylether (as mentioned above for compound **7**) using copper triphenylphosphine bromide, diisopropylethylamine and *N*,*N*-dimethylformamide as a solvent at 50 °C for 16 h to afford G2 click product **12** in 64% yield.

The acetal protecting groups were removed in 83% yield by refluxing with an acidic ion-exchange resin dowex in methanol to obtain the water-soluble core−shell architecture **13**. The eight hydroxyl groups of the G2 click amphiphile **13** were then completely esterified, again by using *N*-Boc-glycine as the acylating agent in the presence of EDCI and DMAP at room temperature in DMF solvent to furnish octa boc-protected compound **14** in 70% isolated yield. Octa boc-protected compound **14** was then treated overnight with a mixture of trifluoroacetic acid/dichloromethane (1:3) to afford octaaminated amphiphile (G2-octaamine) **4**, in quantitative yield as trifluoroacetate salt (Scheme 2).

In order to investigate that the siRNA complexation ability of the glycine functionalized amphiphiles **1**−**4** was indeed due to the combined effect of the hydrophobic alkyl chain and the hydrophilic glycine functionalized dendrons, we also synthesized a reference dendron **16** having two surface amino groups and without having a C-18 alkyl chain at the core (Scheme 3). Compound **16** was obtained in quantitative yield by the deprotection of boc-groups of compound **15**[44] using a mixture of trifluoroacetic acid/dichloromethane (1:3) (Scheme 3).

Scheme 3. Synthesis of Dendron 16

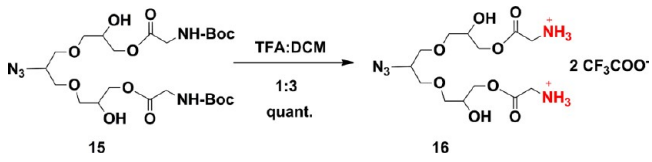

Physico-Chemical Characterization of Amphiphiles. Amphiphilic structures with long alkyl groups form stable aggregates and are therefore useful for transporting e.g. genetic material, particularly if the formed supramolecular architectures exhibit a net positive charge on the surface to complex the negatively charged siRNA. To examine the characteristics of the dendritic amphiphiles to be compared, the aggregation behavior as well as the size and zeta potential were studied using different physical characterization methods such as fluorescence spectroscopy, DLS, and zeta potential measurements.

Initially, the aggregation behavior of the four amphiphiles was studied by means of fluorescence spectroscopy employing hydrophobic fluorescent dye DPH in HEPES saline buffer solution.[37−40] It is known that above a particular concentration, called the critical micelle concentration (CMC), amphiphilic molecules self-associate to form thermodynamically stable micellar aggregates.[37−40] We have chosen a neutral fluorescent probe (DPH) for the determination of CMC's so as to avoid undesirable ionic interactions with our positively charged amphiphiles. At concentrations below CMC, DPH exists predominantly in an aqueous environment and exhibits low fluorescence. Formation of micelles results in the preferential partitioning of the DPH into the hydrophobic interior of the micelles with a concomitant sharp increase in fluorescence. Figure 2 shows that as the concentration of the amphiphile is increased, fluorescence is weak at the lowest concentrations, then rises (first end-point), and finally increases sharply (second end-point). This is interpreted as follows: The first rise in fluorescence (first end-point) occurs at the premicellar concentration by the formation of small aggregates between the probe molecule and the surfactant, and the second rise in fluorescence (second end-point) occurs at and above the CMC of the amphiphile. As the amount of amphiphile is increased, the number of micelles and the amount of bound DPH increase, so that fluorescence also increases. The CMC is given by the intersection of the straight line through the fluorescence at low detergent concentrations with a straight line through the fluorescence values in the region of rapid intensity increase. The determined CMC values, given in Table 1, showed that all four amphiphiles aggregate at a micromolar level ranging from 10 to 60 μM. The CMC values are comparable to our

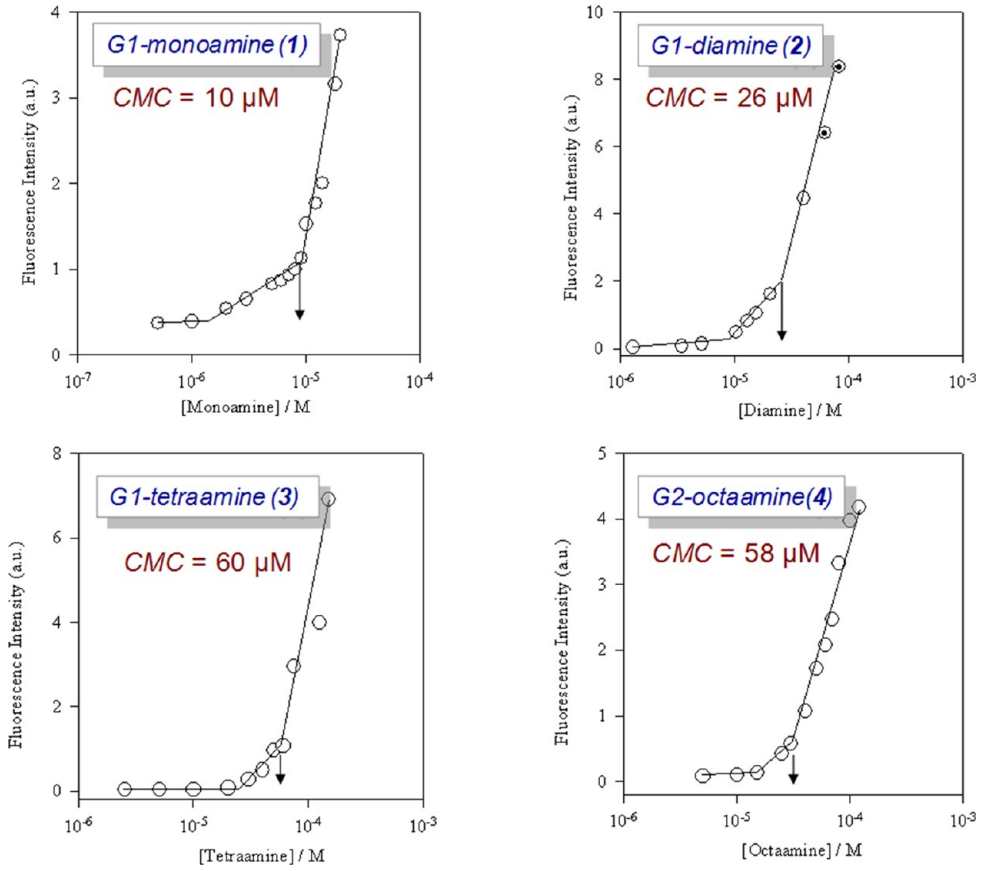

Figure 2. Determination of CMC of glycine amphiphiles in 0.5 μM DPH (aqueous HEPES saline (pH 7.2, 9.4 mM NaCl).

Table 1. CMC, Size, and Zeta-Potential of the Synthesized Glycine Amphiphiles

amphiphile	CMC[a] [μM]	size[a,b] (solo) d_H [nm]	ζ-potential[a] (solo) [mV]
G1-monoamine (**1**)	10	8.4 (±0.3)	57.3 (±0.4)
G1-diamine (**2**)	26	7.3 (±0.4)	40.1 (±3.2)
G1-tetraamine (**3**)	60	6.4 (±0.2)	47.5 (±2.7)
G2-octaamine (**4**)	58	8.2 (±0.9)	58.1 (±1.3)
DNA			−41

[a]Micellar dispersions in HEPES saline buffer (pH 7.2, 9.4 mM NaCl). T = 25 °C. [b]Size-distribution by DLS (by volume), PDI = ~0.3−0.5.

previously reported nonionic derivatives[36] using also PG-derived, hydrophobically modified amphiphiles.

The observed variations of up to 1 order of magnitude can be attributed to the fact that cationic amphiphiles typically exhibit higher CMC values due to repulsion forces induced by the incorporated charged moieties in the headgroup of the amphiphiles. Also, the CMC values increased from G1-monoamine (**1**) to G1-tetramine (**3**) which is in accordance considering the number of positive charges which induces more repulsion in the head groups. In order to achieve a good signal-to-noise ratio the concentration of DPH was kept constant (0.5 μM) and adjusted according to the CMCs of the amphiphiles. In this context, it of interest to note that the critical micelle concentration for probe molecules that are incorporated in the micelles may be dependent on the concentration and the size of the probe molecules. Hence, the presence of DPH might affect the aggregation process and disturb the micellar aggregates. However, this effect appears to be of minor importance with regard to the concentration of DPH employed here.[38−40]

The size (hydrodynamic diameter) of the aggregates and their relative size distribution (PDI: polydispersity index) were determined by means of dynamic light scattering (DLS) measurements in HEPES saline buffer (pH 7.2, 2 mM HEPES, 9.4 mM NaCl). As shown in Table 1, all four amphiphiles formed small micelles in the range of 7−9 nm. The hydrodynamic diameters of all four micellar aggregates measured by DLS (7−9 nm) correlate very well with the theoretical value of around 6−8 nm, since the Z-average value displays the size of the micelle including its hydrodynamic water shell, which is slightly larger than the pure amphiphile size by definition (3−4 nm). The corresponding graphs are shown in the Supporting Information as Figure S3.

According to the conducted zeta potential measurements (Table 1), all four micellar constructs showed positive charges within a range of 40−58 mV. This can be attributed to the large number of cationic amine groups, which are most probably located at the surface of the micellar aggregates. Interestingly, G1-monoamine (**1**) has shown maximum positive charge on the surface which could be due to less repulsion of positive charge on the surface of G1-monoamine (**1**).

DNA Binding and Condensation. The process of binding and condensation of DNA represents a prerequisite of nonviral gene therapy, since it facilitates the cellular uptake of the genetic material.

Complexation through cationic carriers is mainly based on electrostatic interactions between the opposite charges of the DNA and the gene vehicle. Cationic complexes are favored by cell membranes owing to negatively charged membrane

components, thus encouraging cell surface binding through electrostatic interactions. We used double-stranded DNA with 21 base pairs instead of siRNA as a model compound to evaluate the gene binding affinities of the dendritic structures.

The DNA binding and complexation properties of the glycine loaded amphiphiles **1**−**4** were initially studied with an EthBr displacement assay. This assay utilizes the competition between the DNA binding ligands and EthBr for binding to DNA. EthBr exhibits intense fluorescence when bound to DNA, but when it is displaced from the DNA by a DNA-binding ligand, its fluorescence is quenched. Notably, the fluorescence of EthBr can increase again if reintercalation in DNA becomes possible. Binding values are best described by CE_{50} values, which report the relevant N/P ratio indicating the nominal dendron charge excess causing a 50% decrease in fluorescence intensity. The concentration of dendritic amphiphile required for effective DNA binding can also be calculated (C_{50}).

We studied the DNA-binding properties at low salt concentration in HEPES saline buffer (pH 7.2, 2 mM HEPES, 9.4 mM NaCl). The data shown in Table 2 demonstrate that all of our four glycine loaded amphiphiles effectively bind to DNA although G1-tetraamine (**3**) had the highest DNA binding affinity in comparison to the CE_{50} as well as the C_{50} values of all tested amphiphiles, since already at a N/P ratio of 0.8 (CE_{50}) fifty percent of the ethidium bromide intercalated in the DNA could be replaced. In addition, a positive trend within the G1 derivatives from the relevant monoamine to the fully substituted tetraamine is noticeable, which clearly can be attributed to multivalency effects. Hence, within this testing series G1-monoamine (**1**) has the lowest ability to bind DNA (CE_{50} = 1.3). Interestingly, G2-octaamine (**4**) did not show better results (CE_{50} = 1.3) than their G1 analogues, even though this would have been expected when considering multivalent aspects. In fact, only in concentration terms, the performance of G2-octaamine (**4**) (C_{50} = 0.8 μM) is relatively comparable to that of G1-tetraamine (**3**) (C_{50} = 0.5 μM), even though the former has eight surface positive charges and the latter has only four.

Table 2. DNA Binding Data Extracted from EthBr Displacement Assays Using HEPES Saline Buffer (pH 7.2, 9.4 mM NaCl)

amphiphile	CE_{50}[a] value	C_{50} value[b] [μM]
G1-monoamine (**1**)	1.3	3.3
G1-diamine (**2**)	1.0	1.3
G1-tetraamine (**3**)	0.8	0.5
G2-octaamine (**4**)	1.3	0.8

[a]CE_{50} represents the charge excess (N/P ratio) required to decrease EthBr fluorescence by 50%. [b]C_{50} represents the concentration of amphiphile required to displace 50% of EthBr.

Thus, it can be concluded that G1-tetraamine (**3**) is the most effective DNA binder in terms of the CE_{50} parameter, which reflects the relative ability of the cationic amine groups to bind anionic DNA. The corresponding titration graphs are shown in the Supporting Information in Figure S2.

Furthermore, we confirmed that the DNA complexation ability of the glycine functionalized amphiphiles **1**−**4** was indeed due to the combined effect of the hydrophobic alkyl chain and the hydrophilic glycine functionalized dendrons, since the dendron **16** alone did not led to any DNA binding effect. As revealed from the Ethbr displacement assay (data not shown), dendron **16** was not able to displace even 20% of the Ethbr from the DNA even at an N/P ratio of 5, thus revealing no complexation ability. The combined effect of the hydrophobic alkyl chain and the cationic hydrophilic glycine functionalized dendron was able to impart **1**−**4** with a strong capacity to form stable self-assembled complexes with DNA and effectively displace Ethbr from the DNA, thus giving good binding values (CE_{50}) in the range of 0.8−1.3. This indicates that the alkyl chain considerably favors the DNA/vector assembly and increases their stability via hydrophobic interactions.

The surface charge of the dendron−DNA polyplexes was then evaluated by zeta-potential (ζ) measurements (see Table 3), which were carried out at 9.4 mm NaCl concentration to allow accurate measurements. We have used double-stranded DNA with 21 base pairs for zeta-potential (ζ) measurements as well. Negative ζ potentials close to −41 mV were observed for free DNA (see Table 1).

The obtained ζ potentials of the polyplexes showed the general trend that, along with rising N/P ratios, the ζ potential increases, which is in complete agreement with theoretical expectations. All four amphiphilic constructs showed positive ζ potentials in the range of 20−43 mV at N/P 10. However, only G1-monoamine (**1**) and G1-diamine (**2**) derived micelles exhibited positive net charges at the N/P ratio of 5 as well.

In addition, the size of amphiphile-DNA polyplexes of different N/P ratios were analyzed by dynamic light scattering (DLS) measurements in order to provide insight into the dimensions of the formed polyplexes which later on should be internalized by the cells, thereby facilitating nucleic acid delivery. We have used double-stranded DNA with 21 base pairs for DLS studies as well. Generally, two different N/P ratios were tested: N/P 5 and 10 (see Table 3). The hydrodynamic diameters, ranging from approximately 69−306 nm at N/P ratio 10, were obtained for all four amphiphiles tested, whereas large aggregates in the range of 212−1383 nm were observed at N/P ratio 5. The corresponding DLS graphs are shown in Supporting Information as Figures S4 and S5.

Table 3. Size and Zeta-Potential of the Glycine Amphiphiles−DNA Polyplexes at Different N/P Ratios

	size (d_H)[a] [nm]		ζ-potential [mV]	
amphiphile	N/P 5	N/P 10	N/P 5	N/P 10
G1-monoamine (**1**)	211.8 (±10.4)	141.1 (±2.8)	+26.5 (±0.9)	+43.1 (±1.3)
G1-diamine (**2**)	1249 (±36.9)	80.7 (±0.5)	+4.9 (±0.1)	+37.9 (±1.1)
G1-tetraamine (**3**)	1383 (±51.3)	68.9 (±0.8)	−12.0 (±1.5)	+42.3 (±0.6)
G2-octaamine (**4**)	1181 (±12.0)	305.9 (±2.8)	−10.2 (±2.6)	+20.6 (±3.9)

[a]Amphiphile−DNA polyplexes in HEPES saline buffer (pH 7.2, 9.4 mM NaCl). T = 25 °C. Size-distribution by DLS (by volume), PDI = ∼0.1−0.3.

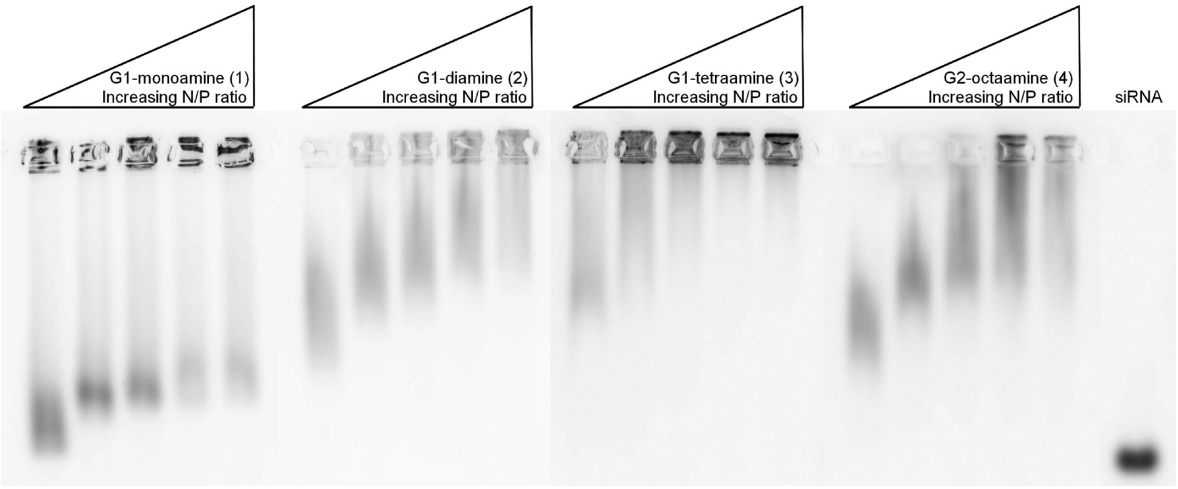

Figure 3. Binding capacity and migration assay of glycine amphiphiles-FAM-siRNA complexes by agarose gel electrophoresis. G1-monoamine (**1**), G1-diamine (**2**), G1-tetraamine (**3**), and G2- octaamine (**4**) are shown with increased N/P ratios (20, 50, 70, 90, and 100) complexed with FAM-labeled siRNA. Complex-free FAM-siRNA is illustrated in the last slot on the right. Images were acquired by detecting the green fluorescence signal.

The binding capacity of all glycine amphiphiles was further demonstrated using agarose gel electrophoresis retardation assay, which directly measures siRNA-dendron interactions. For this purpose, we used FAM-labeled siRNA. As a sign of successful siRNA neutralization and compaction, the constructs (amphiphiles) should either reduce or completely retard the electrophoretic mobility of siRNA. As shown in Figure 3, all glycine amphiphiles exhibited enhanced binding capacity with increased N/P ratios while monoamine was the most inefficient. The complexes of FAM-siRNA with tetraamine mostly remained in the slots indicating proper binding of siRNA molecules. Di- and octaamine derivatives possessed similar and moderate binding capacities as shown by migration assays. Complex-free FAM-siRNA was loaded as migration control. The results were visualized by detecting the green fluorescence signal.

Thus, from the nucleic acids complexation studies it could be concluded that all four glycine functionalized amphiphiles (**1**−**4**) were successfully able to complex nucleic acids with high affinities. Tetraamine was found to be the best DNA binder.

Cytotoxicity and siRNA Transfection Results. The cytotoxic effect of each glycine amphiphile for N/P ratios 20, 50, and 100 was tested by WST-1 assays and xCELLigence (Figure 4) using HeLa cells. The results of WST-1 assays pointed out high toxicity of (A) G1-monoamine (**1**) with N/P ratios higher than 50 and of (B) G1-diamine (**2**) using N/P 100. (C) G1-tetraamine (**3**) and (D) G2-octaamine (**4**) indicated no lethal effects. These findings were confirmed by real-time determination of cell index profiles (E-H) obtained from xCELLigence. The graphs demonstrate the baseline delta cell indexes related to the control cells (control+siRNA, Figure 4). Control cells were incubated with siRNA but without transfection reagent. Incubation with lipofectamine (Figure 4) in comparison with the control cells displayed no difference in cell proliferation over the observed time period.

Table 4 summarizes the outcome of the Cy3-labeled siRNA delivery using the glycine amphiphiles. HeLa cells were transfected with fluorescently labeled siRNA and efficiency of delivery was analyzed after 48 h by fluorescence microscopy. G1-monoamine (**1**) and G1-diamine (**2**) showed positive uptake of labeled siRNA using a ratio of N/P 20. Higher N/P ratios at 50 and 100 caused cytotoxic effects. Intracellular transfer of siRNA with G1-tetraamine (3) was effective at all investigated N/P ratios.

G2-octaamine (**4**) also turned out to be an efficient nanotransporter for fluorescently labeled siRNA at ratios higher than N/P 20 (Table 4). Lipofectamine was used as a control transfection reagent and showed efficient uptake in all experiments.

Further functional analysis of all glycine amphiphiles was performed by investigating the knockdown of normalized luciferase activity in HeLa cells constitutively expressing the luciferase gene. Figure 5 illustrates normalized luciferase knockdown using (A) G1-monoamine (**1**), (B) G1-diamine (**2**), (C) G1-tetraamine (**3**), and (D) G2-octaamine (**4**) at N/P ratios of 20, 50, 70, 90, and 100 for luciferase specific siRNA delivery after 48 h.

The relative luminescence was determined by measuring the luciferase activity per living cell relative to the Calcein AM signal. This approach provided a simultaneous measure for transfection efficiency and cytotoxicity of investigated nanotransporters within the same assay. This experiment revealed that both G1-mono-(**1**) and diamine (**2**) are both toxic independently of investigated N/P ratio compared with control cells. Both the control+siRNA and control were without transfection reagent. G1-monoamine (**1**) at a ratio of N/P 20 exhibited low knockdown of luciferase in comparison to the transfection data of nontargeting (nT) siRNA while diamine showed no obvious downregulation. Transfections with G1-tetraamine (**3**) up to N/P 70 led to luciferase knockdown while increased N/P ratios at 90 and 100 caused toxic effects. G2-octaamine (**4**) had no toxic impact on cells and exhibited the most efficient combination of low toxicity and high knockdown efficiency regarding the entire spectrum of investigated N/P ratio.

Furthermore, the toxicity of G2-octaamine (**4**) complexed with siRNA was tested in vivo by intravenous administration. No significant increase in the tested proinflammatory cytokine levels compared to the control was detected in the serum reflecting the nontoxic effect of G2-octaamine (**4**) detected in vitro (see the Supporting Information, Figure S6).

The knockdown of GAPDH after siRNA delivery in HeLa cells was proven by RT-qPCR (Figure 6). Due to the cytotoxic effects caused by G1-monoamine (**1**), G1-diamine (**2**) and G1-

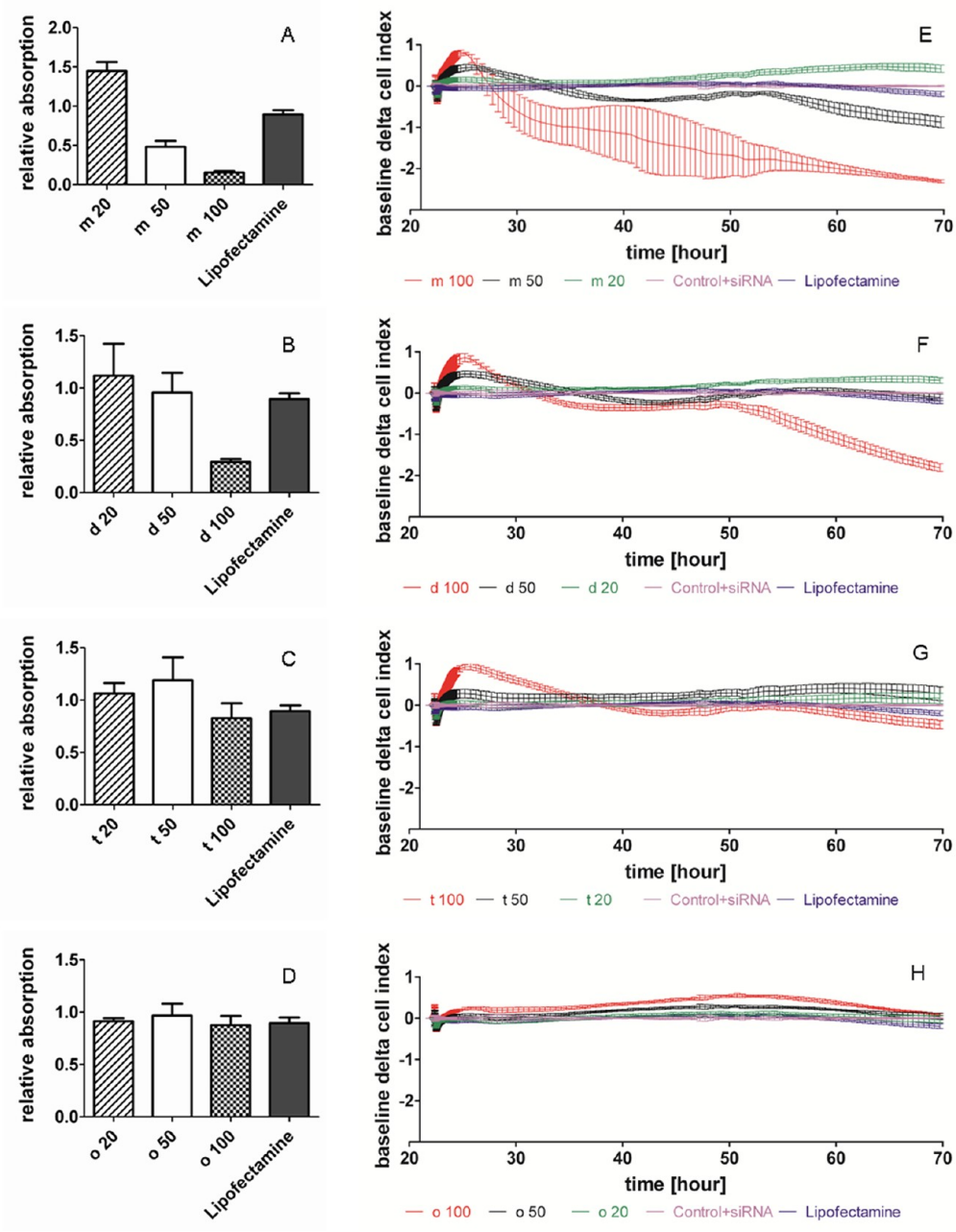

Figure 4. Cytotoxicity by WST-1 assay and xCELLigence (Roche). (A–D) Results of WST-1 assay and (E–H) of xCELLigence with nontargeting siRNA transfected HeLa cells. G1-monoamine (**1**) is shown in panels A and E, G1-diamine (**2**) in B and F, G1-tetraamine (**3**) in C and G, and G2-octaamine (**4**) in D and H. The N/P ratios 20, 50, and 100 were tested. Cells treated with siRNA and without transfection reagent were used as reference. Lipofectamine was used as a control transfection reagent.

Table 4. Cy3-Labeled siRNA Delivery with Glycine Amphiphiles (+ = Successful, − = Failed)

amphiphile	N/P 20	N/P 50	N/P 100
G1-monoamine (**1**)	+	toxic	toxic
G1-diamine (**2**)	+	toxic	toxic
G1-tetraamine (**3**)	+	+	+
G2-octaamine (**4**)	−	+	+

tetraamine (**3**) at high N/P ratios, the results of respective knockdown experiments are shown for N/P ratio 20 and for G2-octaamine (**4**) N/P 20, 50, and 100. No significant downregulations were observed by N/P 20 for all glycine amphiphiles. GAPDH possessed 60% downregulation in experiments using G2-octaamine (**4**) at a ratio of N/P 50. Knockdown efficiency of Lipofectamine was around 50%. Increased nonspecific knockdown was observed for G2-octaamine (**4**) with N/P 20, 50, and 100, which is evidence of an increase in the cytotoxicity from the polyplexes.

After observing the successful luciferase and GAPDH gene silencing using G2-octaamine (**4**), we recorded the size and zeta-potential of the polyplexes of G2-octaamine (**4**) and siRNA (ON-TARGETplus GAPD Control siRNA, D-001830-01, Thermo Fisher Scientific) at different N/P ratios in aqueous HEPES saline buffer (9.4 mM NaCl, pH 7.4). We observed the size of the G2-octaamine (**4**)-siRNA polyplex to be around 118.4 ± 1.7 at an N/P ratio of 50 (see Table S1 in the

dx.doi.org/10.1021/bm300892v | *Biomacromolecules* 2012, 13, 3087–3098

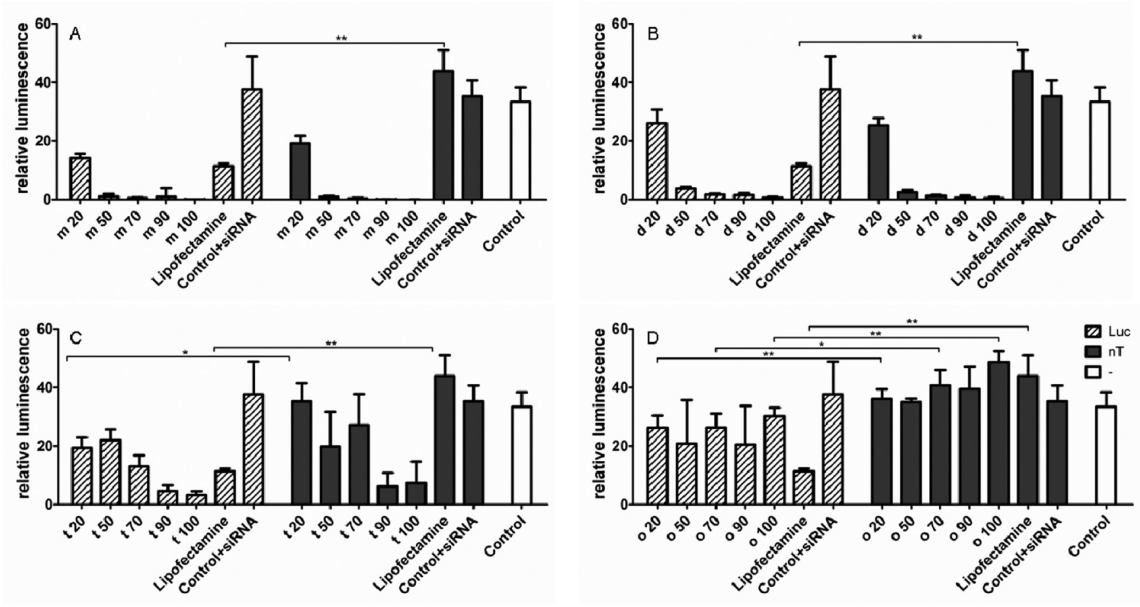

Figure 5. Normalized luciferase assay of HeLa-Luc cells. HeLa-Luc cells were transfected with luciferase specific and nontargeting (nT) siRNA for 48 h. The results pointed out the relative luminescence for (A) G1-monoamine (**1**), (B) G1-diamine (**2**), (C) G1-tetraamine (**3**), and (D) G2-octaamine (**4**) at N/P ratios of 20, 50, 70, 90, and 100. Outcomes of controls (cells with and without siRNA) and transfections with Lipofectamine are represented in each figure. The normalization was performed using data of simultaneous Calcein AM measurement. (Statistical data by paired *t* test; * $p < 0.05$, ** $p < 0.01$.)

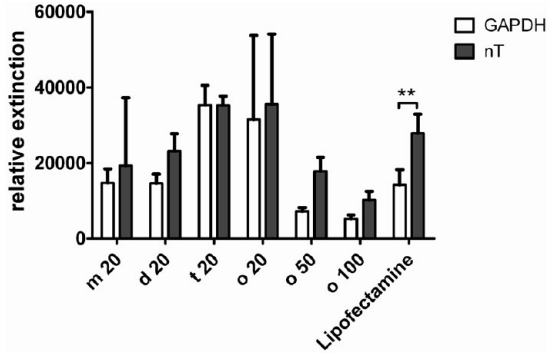

Figure 6. Quantification of GAPDH mRNA by RT-qPCR. Values of relative knockdown of GAPDH transcripts are shown after 48 h of transfection with GAPDH specific and nontargeting (nT) siRNA in HeLa cells. The data show the results of G1-monoamine (**1**), G1-diamine (**2**), and G1-tetraamine (**3**) with N/P 20 and of G2-octaamine (**4**) with N/P 20, 50, and 100 as well as Lipofectamine as control transfection. (Statistical data by paired *t* test; * $p < 0.05$, ** $p < 0.01$.)

Supporting Information), which suggests that the polyplex at this N/P ratio can be easily internalized by the cell.

CONCLUSIONS

In conclusion, we have developed multivalent oligoglycerol dendron based low molecular weight amphiphiles with well-defined molecular structures that express controlled glycine arrays on their surfaces. In this study, we have controlled the loading of amine content on the surface of the dendritic headgroups, using facile chemo-enzymatic and chemical synthetic routes. We studied the structure−activity relationships with respect to the siRNA/DNA complexation, toxicity, and transfection profiles with the synthesized polycations. Our findings disclose that a higher number of amine functionalities (glycine loading) on the surface of dendritic headgroup make the vector more efficient in terms of siRNA transfection and cytotoxicity. Furthermore, we found that a second-generation amphiphilic dendrimer (G2-octaamine, **4**) with eight amine groups on its surface and a hydrophobic C-18 alkyl chain at the core, acts as an efficient vector to deliver siRNA inside the cell and achieved potent gene silencing as demonstrated by the knockdown of normalized luciferase activity and also for GAPDH in HeLa cells. The amphiphilic vector is nontoxic even at higher ratio of N/P 100 both in vitro and in vivo. To the best of our knowledge, this is the first example of successful in vitro siRNA transfection using dendritic amphiphiles. It may serve as a new promising alternative for nonviral siRNA delivery system and be useful for further applications in nanobiotechnology.

ASSOCIATED CONTENT

Supporting Information

^{1}H and ^{13}C NMR spectra of compounds **9**, **3**, **14**, and **4**. Graphs and data for the physicochemical characterization of compounds **1**−**4** and also for their polyplexes with DNA and siRNA, and the in vivo toxicity graphs for compound **4**-siRNA polyplex. This material is available free of charge via the Internet at http://pubs.acs.org.

AUTHOR INFORMATION

Corresponding Author

*(R.H.) Phone: +49-30-838-52633. Fax: +49-30-838-53357. E-mail: haag@chemie.fu-berlin.de. Website: http://www.polytree.de. (R.E.) Phone: +49-30-838-62575. Fax: +49-30-838-62584. E-mail: einspani@zedat.fu-berlin.de.

Notes

The authors declare no competing financial interest.

■ ACKNOWLEDGMENTS

The authors acknowledge the support from the Biotransporter project of the Bundesministerium für Bildung und Forschung (BMBF).

■ REFERENCES

(1) Zhang, X.; McIntosh, T. J.; Grinstaff, M. W. *Biochimie* **2012**, *94*, 42−58.
(2) Cavazzana-Calvo, M.; Hacein-Bey, S.; De.Saint Basile, G.; Gross, F.; Yvon, E.; Nusbaum, P.; Selz, F.; Hue, C.; Certain, S.; Casanova, J. L.; Bousso, P.; Le Deist, F.; Fischer, A. *Science* **2000**, *288*, 669−672.
(3) Yang, Z. R.; Wang, H. F.; Zhao, J.; Peng, Y. Y.; Wang, J.; Guinn, B.-A.; Huang, L. Q. *Cancer Gene Ther.* **2007**, *14*, 599−615.
(4) Niven, R.; Pearlman, R.; Wedeking, T.; Mackeigan, J.; Noker, P.; Simpson-Herren, L.; Smith, J. G. *J. Pharm. Sci.* **1998**, *87*, 1292−1299.
(5) Anderson, W. F. *Nature* **1998**, *392*, 25−30.
(6) Verma, I. M.; Somia, N. *Nature* **1997**, *389*, 239−242.
(7) Felgner, P. L.; Gadek, T. R.; Holm, M.; Roman, R.; Chan, H. W.; Wenz, M.; Northrop, J. P.; Ringold, G. M.; Danielsen, M. *Proc. Natl. Acad. Sci. U.S.A.* **1987**, *84*, 7413−7417.
(8) Fukushima, S.; Miyata, K.; Nishiyama, N.; Kanayama, N.; Yamasaki, Y.; Kataoka, K. *J. Am. Chem. Soc.* **2005**, *127*, 2810−2811.
(9) Harada, A.; Kawamura, M.; Matsuo, T.; Takahashi, T.; Kono, K. *Bioconjugate Chem.* **2006**, *17*, 3−5.
(10) Gupta, B.; Levchenko, T. S.; Torchilin, V. P. *Adv. Drug Delivery Rev.* **2005**, *57*, 637−651.
(11) Behr, J. P. *Acc. Chem. Res.* **1993**, *26*, 274−278.
(12) Smith, D. K. *Curr. Top. Med. Chem.* **2008**, *8*, 1187−1203.
(13) Badjic, J. D.; Nelson, A.; Cantrill, S. J.; Turnbull, W. B.; Stoddart, J. F. *Acc. Chem. Res.* **2005**, *38*, 723−732.
(14) Kitov, P. I.; Bundle, D. R. *J. Am. Chem. Soc.* **2003**, *125*, 16271−16284.
(15) Kukowska-Latallo, J.-F.; Bielinska, A. U.; Johnson, J.; Spindler, R.; Tomalia, D. A.; Baker, J. R. *Proc. Natl. Acad. Sci.* **1996**, *93*, 4897−4902.
(16) Turunen, M. P.; Hiltunen, M. O.; Ruponen, M.; Virkamaki, L.; Szoka, F. C.; Urtti, A.; Yla-Herttuala, S. *Gene Ther.* **1999**, *6*, 6−11.
(17) Ohsaki, M.; Okuda, T.; Wada, A.; Hirayama, T.; Niidome, T.; Aoyagi, H. *Bioconjugate Chem.* **2002**, *13*, 510−517.
(18) Fischer, W.; Calderón, M.; Schulz, A.; Andreou, I.; Weber, M.; Haag, R. *Bioconjugate Chem.* **2010**, *21*, 1744−1752.
(19) Ofek, P.; Fischer, W.; Calderon, M.; Haag, R.; Satchi-Fainaro, R. *FASEB J.* **2010**, 3122−3134.
(20) Germershaus, O.; Pickaert, G.; Konrad, J.; Krüger, U.; Kissel, T.; Haag, R. *Macromol. Biosci.* **2010**, *10*, 1055−1062.
(21) Fischer, W.; Calderon, M.; Haag, R. Hyperbranched Polyamines for Transfection. In *Nucleic Acid Transfection*; Springer-Verlag: Berlin, 2010; Vol. *296*, pp 95−129.
(22) Fischer, W.; Quadir, M. A.; Barnard, A.; Smith, D. K.; Haag, R. *Macromol. Biosci.* **2011**, *11*, 1736−1746.
(23) Wan, K.; Ebert, B.; Voigt, J.; Haag, R.; Kemmner, W. *Nanomed. Nanotech. Biol. Med.* **2012**, *8*, 393−398.
(24) Khandare, J.; Calderon, M.; Dagia, N.; Haag, R. *Chem. Soc. Rev.* **2012**, *41*, 2824−2848.
(25) Calderon, M.; Quadir, M. A.; Sharma, S. K.; Haag, R. *Adv. Mater.* **2010**, *22*, 190−218.
(26) Quadir, M. A.; Calderón, M.; Haag, R. *Cancer Drug Delivery*; Wiley-VCH Books: Weinheim, Germany, 2011; pp 513−553.
(27) Lv, H.; Zhang, S.; Wang, B.; Cui, S.; Yan, J. *J. Controlled Release* **2006**, *114*, 100−109.
(28) Kuo, J.-H. S.; Liou, M.-J.; Chiu, H.-C. *Mol. Pharm.* **2010**, *7*, 805−814.
(29) Guillot, M.; Eisler, S.; Weller, K.; Merkle, H. P.; Gallani, J. L.; Diederich, F. *Org. Biomol. Chem.* **2006**, *4*, 766−769.
(30) Barnard, A.; Posocco, P.; Pricl, S.; Calderon, M.; Haag, R.; Hwang, M. E.; Shum, V. W. T.; Pack, D. W.; Smith, D. K. *J. Am. Chem. Soc.* **2011**, *133*, 20288−20300.
(31) Bayele, H. K.; Sakthivel, T.; O'Donell, M.; Pasi, K. J.; Wilderspin, A. F.; Lee, C. A.; Toth, I.; Florence, A. T. *J. Pharm. Sci.* **2005**, *94*, 446−457.
(32) Jones, S. P.; Gabrielson, N. P.; Wong, C.-H.; Chow, H.-F.; Pack, D. W.; Posocco, P.; Fermeglia, M.; Pricl, S.; Smith., D. K. *Mol. Pharm.* **2011**, *8*, 416−429.
(33) Poon, Z.; Lee, J. A.; Huang, S.; Prevost, R. J.; Hammond, P. T. *Nanomedicine* **2011**, *7*, 201−209.
(34) Karmali, P. P.; Chaudhuri, A. *Med. Res. Rev.* **2007**, *27*, 696−722.
(35) Bhattacharya, S.; Bajaj, A. *Chem. Commun.* **2009**, 4632−4656.
(36) Trappmann, B.; Ludwig, K.; Radowski, M. R.; Shukla, A.; Mohr, A.; Rehage, H.; Böttcher, C.; Haag, R. *J. Am. Chem. Soc.* **2010**, *132*, 11119−11124.
(37) Purohit, V. S.; Balasubramanian, S. V. *AAPS J.* **2006**, *8*, E362−370.
(38) Chattopadhyay, A.; London, E. *Anal. Biochem.* **1984**, *139*, 408−412.
(39) Nakahara, Y.; Kida, T.; Nakatsuji, Y.; Akashi, M. *Langmuir* **2005**, *21*, 6688−6695.
(40) Mohr, A.; Talbiersky, P.; Korth, H.-G.; Sustmann, R.; Boese, R.; Bläser, D.; Rehage, H. *J. Phys. Chem. B* **2007**, *111*, 12985−12992.
(41) Kostiainen, M. A.; Smith, D. K.; Ikkala, O. *Angew. Chem.* **2007**, *119*, 7744−7748.
(42) Sharbati, J.; Lewin, A.; Kutz-Lohroff, B.; Kamal, E.; Einspanier, R.; Sharbati, S. *PLoS ONE* **2011**, *6*, e20258.
(43) Vandesompele, J; De Preter, K; Pattyn, F; Poppe, B; Van Roy, N; De Paepe, A; Speleman, F. *Genome Biol.* **2002**, *3*, r0034.1−0034.11.
(44) Malhotra, S.; Calderón, M.; Prasad, A. K.; Parmar, V. S.; Haag, R. *Org. Biomol. Chem.* **2010**, *8*, 2228−2237.
(45) Wyszogrodzka, M.; Haag, R. *Chem.—Eur. J.* **2008**, *14*, 9202−9214.